The Helicase and RNaseIIIa Domains of Arabidopsis Dicer-Like1 Modulate Catalytic Parameters during MicroRNA Biogenesis[1][C][W][OA]

Chenggang Liu[2], Michael J. Axtell, and Nina V. Fedoroff[3]*

Department of Biology, Pennsylvania State University, University Park, Pennsylvania 16802

Dicer-Like1 (DCL1), an RNaseIII endonuclease, and Hyponastic Leaves1 (HYL1), a double-stranded RNA-binding protein, are core components of the plant microRNA (miRNA) biogenesis machinery. *hyl1* null mutants accumulate low levels of miRNAs and display pleiotropic developmental phenotypes. We report the identification of five new *hyl1* suppressor mutants, all of which are alleles of *DCL1*. These new alleles affect either the helicase or the RNaseIIIa domains of DCL1, highlighting the critical functions of these domains. Biochemical analysis of the DCL1 suppressor variants reveals that they process the primary transcript (pri-miRNA) more efficiently than wild-type DCL1, with both higher K_{cat} and lower K_m values. The DCL1 variants largely rescue wild-type miRNA accumulation levels in vivo, but do not rescue the *MIRNA* processing precision defects of the *hyl1* null mutant. In vitro, the helicase domain confers ATP dependence on DCL1-catalyzed *MIRNA* processing, attenuates DCL1 cleavage activity, and is required for precise *MIRNA* processing of some substrates.

MicroRNAs (miRNAs) are sequence-specific guides that direct posttranscriptional suppression of target gene expression. The biogenesis of miRNAs starts with the transcription of *MIRNA* genes by RNA polymerase II (Lee et al., 2004a). The primary transcript, termed the pri-miRNA, contains an imperfect hairpin structure that is sequentially cleaved by RNaseIII family enzymes to release one or more miRNA/miRNA* duplexes (Hutvágner and Zamore, 2002; Lee et al., 2003). The miRNA strand is then incorporated into the RNA-induced silencing complex to form a functional miRNA complex. In animal cells, pri-miRNA processing is spatially separated and performed by two different RNaseIII family enzymes. The first cleavage, which releases an intermediate hairpin structure called the precursor miRNA (pre-miRNA), is typically executed by an RNAseIII protein called Drosha in the nucleus (Lee et al., 2003). The pre-miRNA is then transported to the cytoplasm by Exportin-5 (Yi et al., 2003; Lund and Dahlberg, 2006) and cleaved by another RNAseIII protein called Dicer to generate the miRNA/miRNA* duplex (Lee et al., 2003). By contrast, the processing of plant pri-miRNAs into miRNA/miRNA* duplexes takes place entirely in the nucleus and is typically catalyzed by a single RNAseIII family enzyme, Dicer-Like1 (DCL1; Reinhart et al., 2002; Kurihara and Watanabe, 2004; Park et al., 2005; Fahlgren et al., 2007).

Although Arabidopsis (*Arabidopsis thaliana*) expresses other DCL proteins, DCL1 is the primary enzyme involved in miRNA biogenesis (Kurihara and Watanabe, 2004; Fahlgren et al., 2007). Besides DCL1, several other accessory proteins are also involved in plant miRNA biogenesis, including Hyponastic Leaves1 (HYL1), a double-stranded (ds)RNA-binding protein, and Serrate (SE), a C_2H_2 zinc finger protein. The null mutant of *hyl1* and a hypomorphic mutant of *se* exhibit low miRNA levels (Han et al., 2004; Vazquez et al., 2004; Lobbes et al., 2006; Yang et al., 2006; Laubinger et al., 2008). HYL1 and SE form complexes with DCL1 in vivo (Fang and Spector, 2007; Song et al., 2007) and enhance the in vitro DCL1 processing rate and accuracy (Dong et al., 2008). These observations suggest that HYL1 and SE function to modulate DCL1 activity. Besides HYL1 and SE, Dawdle (an FHA domain protein) and two nuclear cap-binding proteins (CBP20 and CBP80) also affect miRNA biogenesis (Kim et al., 2008; Laubinger et al., 2008; Yu et al., 2008). Dawdle has been proposed to participate in miRNA biogenesis by facilitating DCL1 access to pri-miRNA (Yu et al., 2008), while CBP20 and CBP80 may mediate the interaction between the nuclear Cap-binding complex and the miRNA processing machinery (Laubinger et al., 2008; Yu et al., 2008).

The DCL1 domain structure is a typical one for Dicer proteins, consisting of a DExD/H-box RNA helicase

[1] This work was supported by the U.S. National Science Foundation (grant nos. 0718051 to M.J.A. and 0640186 to N.V.F.).

[2] Present address: Plant Biology Division, Samuel Roberts Noble Foundation, Ardmore, OK 73401.

[3] Present address: King Abdullah University of Science and Technology, Thuwal 23955–6900, Saudi Arabia.

* Corresponding author; e-mail nvf1@psu.edu.

The authors responsible for distribution of materials integral to the findings presented in this article in accordance with the policy described in the Instructions for Authors (www.plantphysiol.org) are: Michael J. Axtell (mja18@psu.edu) and Nina V. Fedoroff (nvf1@psu.edu).

[C] Some figures in this article are displayed in color online but in black and white in the print edition.

[W] The online version of this article contains Web-only data.

[OA] Open Access articles can be viewed online without a subscription.

www.plantphysiol.org/cgi/doi/10.1104/pp.112.193508

domain, a DUF283 domain, which has recently been annotated as a novel RNA-binding domain (Qin et al., 2010), a PAZ domain, two tandem RNaseIII domains (RNaseIIIa and RNaseIIIb), and two tandem dsRNA-binding domains (Fig. 1A). Complete loss of *DCL1* function results in embryonic lethality in Arabidopsis (Schauer et al., 2002; Nodine and Bartel, 2010). Genetic studies have identified several nonnull, nonlethal *dcl1* alleles. *dcl1-7* and *dcl1-8* have point mutations in the helicase domain and accumulate lower levels of miRNA than wild-type plants, implying that the helicase domain is critical for miRNA biogenesis (Kasschau et al., 2003; Kurihara and Watanabe, 2004; Mlotshwa et al., 2005). *dcl1-9*, which harbors a T-DNA insertion in the last dsRNA-binding domain, and *dcl1-15*, which has a point mutation in the catalytic site of the RNAseIIIb domain, also accumulate reduced levels of miRNAs (Kurihara and Watanabe, 2004; Kurihara et al., 2006; Willmann et al., 2011). Another allele with a lesion in the helicase domain, *dcl1-13*, was identified as a semidominant suppressor of *hyl1* (Tagami et al., 2009). Unlike the hypomorphic *dcl1* alleles, *dcl1-13* is a gain-of-function allele. It promotes miRNA processing in the absence of HYL1, but impairs miRNA processing in the presence of HYL1 (Tagami et al., 2009).

In this study, we identified five new alleles of *dcl1* based on a screen for suppressors of the null *hyl1-2* mutant. One allele has a mutation in the coding sequence for the helicase domain, while the other four mutations affect the sequence encoding the RNaseIIIa domain. miRNA accumulation is restored to nearly wild-type levels in *hyl1-2*/*dcl1* double mutants, but the *MIRNA* processing accuracy defects caused by lack of *HYL1* function persist. Biochemical characterization of the mutant DCL1 enzymes revealed that both helicase- and RNaseIIIa-mutated suppressor variants of DCL1 process pri-miRNA more efficiently than the wild-type enzyme. Moreover, the helicase domain of DCL1 is responsible for the ATP dependence of *MIRNA* processing, attenuates the DCL1 cleavage activity of certain substrates, and contributes to the accurate *MIRNA* processing of others. Finally, we show that DCL1 cleaves pri-miRNA transcripts processively.

RESULTS

DCL1 Alleles That Suppress the *hyl1-2* Phenotype

hyl1-2 is a null allele that harbors a T-DNA insertion in the sequence encoding the first dsRNA-binding domain (Han et al., 2004; Vazquez et al., 2004). To obtain mutations that suppress the *hyl1-2* mutant phenotype, we ethyl methanesulfonate mutagenized about 6,000 *hyl1-2* seeds and screened 110 pools (about 50 plants per pool) of M_2 plants. The *hyl1-2* mutation is pleiotropic; mutant plants exhibit leaf hyponasty, smaller stature, and reduced fertility, among other phenotypes (Lu and Fedoroff, 2000). The leaves of 4- to 5-week-old *hyl1-2* plants are markedly upward curled (Fig. 1B), hence we screened for plants with wild-type leaves. In total, we obtained six lines showing heritable normalization of the *hyl1* leaf phenotype, albeit to different extents (Table I; Fig. 1B).

To identify the mutated genes, we crossed each of the six suppressor mutants with wild-type plants and generated segregating F2 populations. None of these F2 populations yielded segregants displaying the *hyl1-2* leaf phenotype, suggesting that the suppressors are both linked to the *HYL1* locus and dominant. *HYL1* and *DCL1* are both on chromosome 1, approximately 10 cM apart. In view of the fact that a previously reported *hyl1-2* suppressor screen resulted in the isolation of a dominant *DCL1* suppressor mutation (Tagami et al., 2009), we sequenced the *DCL1* locus in all six suppressor lines. We found that all six harbored missense mutations within the *DCL1* gene (Table I), two of which were identical. Thus we obtained five new *hyl1-2* suppressor alleles of *DCL1* and designated them *dcl1-20*, *dcl1-21*, *dcl1-22*, *dcl1-23*, and *dcl1-24* (Table I). The extent of phenotypic recovery varied among the alleles, with *dcl1-20* and *dcl1-21* displaying the most complete phenotypic suppression, while the *dcl1-23* allele showed weaker suppression (Fig. 1B).

Four of the five alleles (*dcl1-21* through *-24*) have mutations in the first RNAaseIII domain (RNaseIIIa), while the fifth (*dcl1-20*) has a mutation in the N-terminal helicase domain (Fig. 1A). The alignment of Arabidopsis DCL1 with other plant DCL proteins showed that the amino acid residue changed in the *dcl1-20* allele is highly conserved among all of these proteins, while the mutated positions in the RNaseIIIa domain are conserved among plant DCL1 proteins, but less so among other DCL proteins (Supplemental Fig. S1). Similar to *dcl1-13*, which has a suppressor mutation near the DECH signature motif (DExH/D domain, Walker B motif; Tagami et al., 2009), the mutation in the *dcl1-20* allele is close to the DExH/D Walker B motif, suggesting these positions are crucial for the activity of the helicase domain (Supplemental Fig. S1). The DExH/D motif is a highly conserved domain that coordinates the magnesium ion in the NTPase catalytic center (Rocak and Linder, 2004). Since the mutations in *dcl1-21*, *dcl1-22*, *dcl1-23*, and *dcl1-24* are clustered in the RNaseIIIa domain, we anticipated that these mutations would alter the processing activity of DCL1. Molecular modeling predicts that all of the amino acid substitutions observed in the suppressors affect residues on the surface of DCL1 (Supplemental Fig. S2), as does that in *dcl1-13* (Tagami et al., 2009).

To test whether the observed mutations in *DCL1* are causal in suppressing the *hyl1-2* phenotype, we transformed *hyl1-2* plants with constructs containing each of the five *dcl1* alleles expressed from the native *DCL1* promoter. As controls, we used a wild-type *DCL1* gene and *dcl1-7*, a hypomorphic *DCL1* allele with a mutation in the helicase domain (Kasschau et al., 2003). Between 90% and 100% of the T1 plants transformed with the *dcl1* suppressor alleles did, indeed, suppress the *hyl1-2* phenotype (Fig. 1C). In contrast, none of the

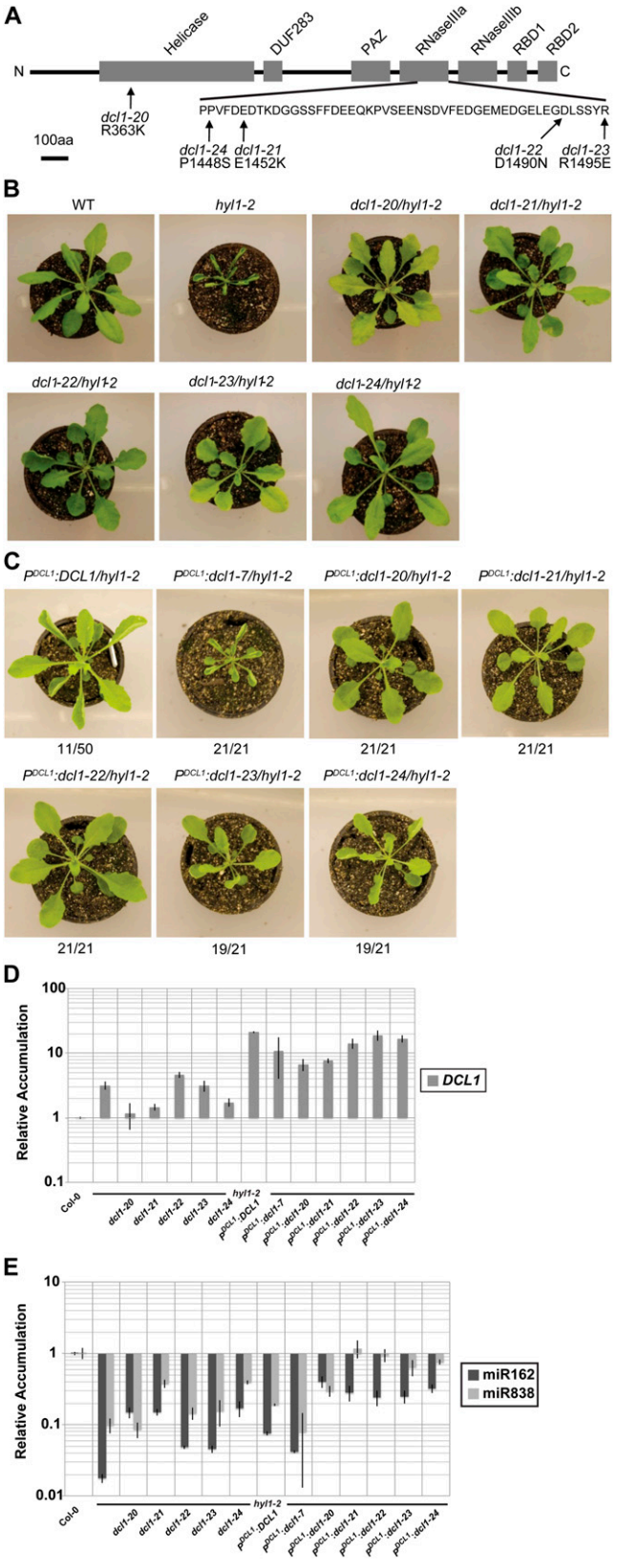

Figure 1. Identification of *dcl1* alleles that suppress the *hyl1-2* phenotype. A, Schematic representation of the DCL1 protein. Labeled boxes indicate protein domains. The positions and amino acid substitutions identified in *dcl1* suppressor alleles are indicated. The RNaseIIIa region is expanded for clarity. B, Photographs of plants showing the phenotypes of *dcl1* mutants that suppress the *hyl1-2* phenotype. Five-week-old plants grown under a 12L/12D light cycle. C, Complementation of *hyl1-2* by *dcl1* suppressor alleles. *hyl1-2* plants were transformed with wild-type *DCL1*, *dcl1-7*, and the indicated *dcl1* suppressor alleles under the control of the native *DCL1* promoter. Numbers indicate the fraction of T1 plants showing the pictured phenotype. D, Quantitative real-time PCR analysis of intact *DCL1* mRNA accumulation. Mean accumulation levels (relative to the mean Columbia-0 value) normalized to *ACTIN2* accumulation, ±1 SD are plotted ($n = 4$; two biological replicates × two technical replicates). Samples were from 25-d-old rosette leaves from long-day-grown plants. Data from transgenics were from pooled, herbicide-resistant T2 individuals that complemented the *hyl1-2* leaf phenotype. E, Quantitative real-time PCR analysis of mature miR162 and miR838 accumulation. As above except normalized to *U6* accumulation levels.

T1 plants transformed with the hypomorphic *dcl1-7* allele suppressed the *hyl1-2* phenotype (Fig. 1C).

Interestingly, a minority (22%) of T1 plants transformed with wild-type *DCL1* also showed suppression of the *hyl1-2* phenotype (Fig. 1C), suggesting that increased dosage of *DCL1*, regardless of the obtained point mutations, could also complement *hyl1-2*. Consistent with this hypothesis, *DCL1* mRNA accumulation was about 10- to 20-fold above wild type in leaves of all of the transgenic lines (Fig. 1D). *DCL1* mRNA accumulation was highest in the minority of P^{DCL1}:*DCL1* transgenic plants that complemented *hyl1-2*. However, increased *DCL1* mRNA expression alone cannot explain *hyl1-2* suppression by our new *DCL1* alleles: Nearly 100% of transgenics expressing *dcl1-20*, *dcl1-21*, *dcl1-22*, *dcl1-23*, and *dcl1-24* complemented *hyl1-2*, compared to only 22% of the transgenics expressing wild-type *DCL1*, despite the approximately equivalent accumulation levels of *DCL1* mRNA. In addition, *DCL1* accumulation was reduced to near wild-type levels in the strongest suppressor lines (*hyl1-2*/*dcl1-20* and *hyl1-2*/*dcl1-21*) and no greater than that in the parental *hyl1-2* background for the other three lines (*hyl1-2*/*dcl1-22*, *hyl1-2*/*dcl1-23*, and *hyl1-2*/*dcl1-24*; Fig. 1D). Taken together, our results confirm that the identified *dcl1* mutations suppress the *hyl1-2* phenotype.

DCL1 is subject to negative feedback regulation by two miRNAs. miR162, whose biogenesis is dependent upon the DCL1 protein, targets the *DCL1* mRNA at a site located at the exon 12-13 junction (Xie et al., 2003). DCL1-catalyzed processing of miR838, whose precursor resides within intron 14 of the *DCL1* precursor mRNA, prevents proper splicing of intron 14, resulting in the accumulation of two prominent, nonproductive RNA fragments (Xie et al., 2003; Rajagopalan et al., 2006). Accumulation of miR162 and miR838 was markedly reduced in the *hyl1-2* mutant (Fig. 1E), consistent with the increased accumulation of intact *DCL1* mRNA seen in that line (Fig. 1D). miR162 and miR838 accumulation was slightly recovered in the five *hyl1-2*/*dcl1* suppressor lines relative to the *hyl1-2* single mutant, but still remained well below wild-type levels

Table I. *Novel dcl1 alleles that suppress the hyl1-2 mutation*

Allele	Genomic Mutation (Counted from the Translation Start Site, AT1G01040.1)	Amino Acid Mutation (AT1G01040.1)
dcl1-20	G1088A	R363K
dcl1-21	G4354A	E1452K
dcl1-22	G4468A	D1490N
dcl1-23	G4484A	R1495E
dcl1-24	C4342T	P1448S

(Fig. 1E). Transgenic lines expressing the *dcl1* suppressor alleles had a much more robust recovery of miR162 and miR838 accumulation levels, while transgenic lines expressing wild-type *DCL1* or the hypomorphic *dcl1-7* allele did not (Fig. 1E). Because the *DCL1* transgenes were cDNA based, they lacked the intron-encoded miR838 locus and thus escaped miR838-mediated feedback control. Hence the recovered levels of miR838 in these lines reflects increased biogenesis of miR838 from the endogenous *DCL1* locus.

Partial Recovery of miRNA Accumulation in *hyl1/dcl1* Suppressor Mutants

Accumulation of many mature miRNAs besides miR162 and miR838 is reduced in *hyl1-2* plants compared to that in wild-type plants (Han et al., 2004; Vazquez et al., 2004). We therefore examined miRNA accumulation in the *hyl1-2/dcl1* double mutants by RNA blotting. As shown in Figure 2A, all miRNAs examined accumulated to higher levels in the *hyl1/dcl1* suppressor plants than in the parental *hyl1-2* mutants, but the levels were still slightly lower than those observed in wild-type plants. The accumulation of trans-acting small interfering (si)RNA siRNA255, whose biogenesis depends upon miR173 (Allen et al., 2005), was also restored. Restoration of miRNA levels was lowest in *dcl1-23*, consistent with its weaker suppression phenotype (Fig. 2A).

To obtain a global overview of miRNA accumulation in suppressor plants, we obtained smallRNAseq data from wild type, *hyl1-2*, and two representative *hyl1/dcl1* suppressor plants (*hyl1-2/dcl1-20* and *hyl1-2/dcl1-21*). Separate RNA samples from all four genotypes were obtained from both rosette leaves and flowers, for a total of eight libraries. This experiment yielded between 14 and 38 million genome-mapped 20- to 24-nt small RNAs per sample (Fig. 2B). The fraction of the genome-mapped small RNA pools that correspond to annotated Arabidopsis *MIRNA* hairpins was substantially lower in *hyl1-2* mutant tissues than in the corresponding wild-type tissues, but significantly higher in the tissues of *hyl1-2/dcl1* double mutants than in the *hyl1* single mutant (Fig. 2B). Examination of individual miRNAs in these small RNA populations also indicated their levels to be generally higher in the *hyl1-2/dcl1* double mutants than those in the parental *hyl1-2* mutant (Fig. 2C). Interestingly, miR162, which directs negative feedback regulation of the *DCL1* mRNA, was among the most strongly down-regulated miRNAs in the *hyl1-2* background and recovered to below-median levels in the suppressor mutants (Fig. 2C). The other *DCL1* negative-feedback-related miRNA, miR838, also accumulated below median levels in all conditions (Fig. 2C). Collectively, our analyses of miRNA accumulation show that the *hyl1-2/dcl1* suppressor plants have miRNA levels approaching those of wild-type plants.

A previously described *hyl1-2* suppressor allele, *dcl1-13*, was reported to promote miRNA processing in the absence of *HYL1*, but impair the miRNA processing at the presence of functional HYL1 (Tagami et al., 2009). To determine whether the newly identified alleles similarly affect miRNA processing in plants having a wild-type *HYL1* allele, we isolated homozygotes of the newly identified *DCL1* alleles with wild-type *HYL1*. Our results show that, in the presence of functional HYL1, *dcl1-20*, *dcl1-22*, *dcl1-23*, and *dcl-24* mutants accumulate slightly more miRNA than wild-type plants, while a *dcl1-21* homozygote accumulates slightly less miRNA than wild type (Supplemental Fig. S3). These results indicated that four of the newly identified alleles are unaffected by *HYL1* function, while one allele resembles the behavior of *dcl1-13*.

MIRNA Processing Precision Is Not Restored in *hyl1/dcl1* Suppressor Mutants

HYL1 plays a crucial role in enhancing the precision of *MIRNA* processing by DCL1 (Kurihara et al., 2006; Dong et al., 2008). SmallRNAseq data from *hyl1-2* mutants were therefore examined to determine whether the *hyl1-2* processing precision defect could be inferred from patterns of sequenced small RNAs derived from known *MIRNA* hairpins. Assessment of miRNA processing precision depends critically upon sequencing depth; hence we focused on the most highly expressed *MIRNA* loci for this analysis. Precision was assessed by computing the ratio of imprecise small RNAs to the total *MIRNA*-matched small RNA pool on each highly expressed hairpin. Imprecise small RNAs were defined as those that did not fall within ±2 bases of the annotated mature miRNA(s) or miRNA*(s) positions. The lower precision of miRNA processing in *hyl1-2* plants was indeed apparent in the smallRNAseq data: *MIRNA* loci in *hyl1-2* plants had a higher ratio of imprecise small RNAs than did wild-type plants (Fig. 3). There was no increase in processing precision in the

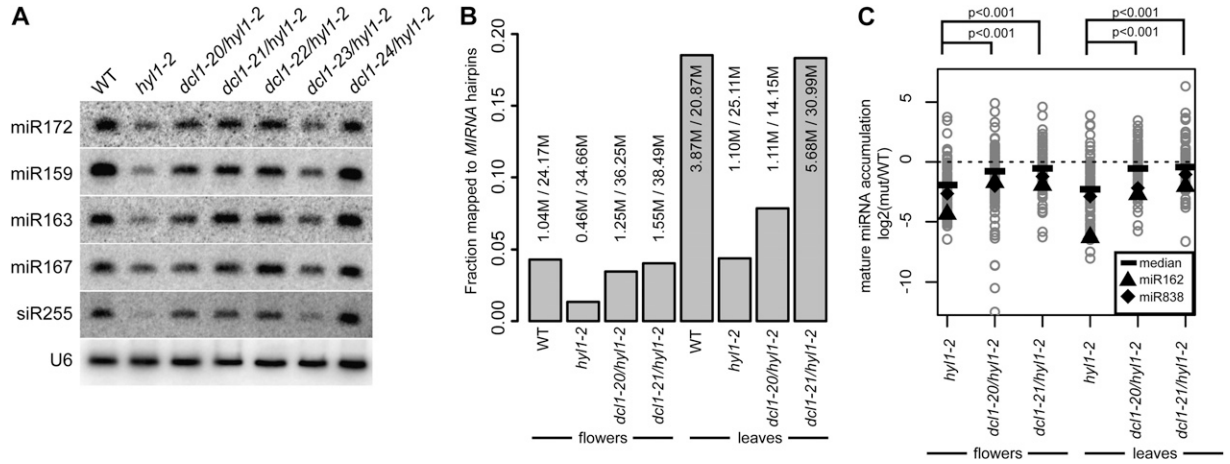

Figure 2. miRNA accumulation in *dcl1/hyl1-2* plants. A, RNA blots for the indicated small RNAs. WT, Wild type. B, Small-RNAseq summary showing the fraction of genome-mapped small RNAs that match *MIRNA* hairpins. C, Relative accumulation of individual mature miRNAs. The $\log_2$-transformed ratios of mutant/wild-type mature miRNA derived from scaled small-RNAseq data were computed for each mutant/wild-type combination and plotted. Thick bars indicate median values for each population. *P* values were derived from Kruskal-Wallis tests. Values corresponding to miR162 and miR838 accumulation are highlighted.

hyl1-2/dcl1 suppressor plants compared to that observed in *hyl1* plants and the imprecisely processed miRNAs were roughly as abundant in suppressor plants as they were in the parental *hyl1-2* single mutant plants (Fig. 3). We conclude that the *dcl1-20* and *dcl1-21* suppressor mutants that bear mutations in the helicase and RNaseIIIa domains, respectively, enhance accumulation of miRNAs in the *hyl1-2* background without alleviating the defect in miRNA processing precision.

Suppressor Variants of DCL1 Have Enhanced Enzymatic Activity

The in vivo data suggest that the suppressor-encoded variants of DCL1 have enhanced enzymatic activity relative to wild-type DCL1. To test this hypothesis, we compared the in vitro processing activities of DCL1 suppressor variants and wild-type DCL1. N-terminal 6-His/C-terminal FLAG-tagged recombinant DCL1, DCL1-20, and DCL1-21 proteins were purified (Supplemental Fig. S4A). 5′-Labeled pri-miRNA156a RNA was used as the substrate in an in vitro processing assay (Supplemental Fig. S5). After incubation with DCL1, the RNA was fractionated by PAGE to resolve RNAs corresponding to both processing intermediates and final products at single nucleotide resolution (Supplemental Fig. S5). Interestingly, this in vitro assay reveals loop to base processing of pri-miRNA156a, a processing mode thought to be relatively rare for plant miRNAs (Addo-Quaye et al., 2009; Bologna et al., 2009). The cleavage rates of the DCL1 enzymes were determined over a range of substrate concentrations. Plots of the initial rate versus the substrate concentration show that the cleavage rates of all DCL1 proteins followed Michaelis-Menten kinetics, indicating the absence of cooperativity between DCL1 proteins (Fig. 4A). As shown in Figure 4B, DCL1-20 and DCL1-21 exhibit lower K_m values and higher K_{cat} values than wild-type DCL1. Consequently, the cleavage efficiencies (calculated as K_{cat} divided by K_m) of DCL1-20 and DCL1-21 were 4.1 and 5.3 times higher than wild-type DCL1, respectively (Fig. 4B). These results show that the suppressor mutations increased both the cleavage activity and the substrate affinity of DCL1. Thus the higher rate of miRNA production by the mutant DCL1 enzymes likely explains their ability to suppress the *hyl1-2* mutant phenotype.

The DCL1 Helicase Domain Attenuates Cleavage Activity and Is Required for the Accurate Processing of pri-miRNA

Previous genetic studies (Kasschau et al., 2003; Kurihara and Watanabe, 2004; Mlotshwa et al., 2005; Tagami et al., 2009) and the isolation of the *dcl1-20* allele highlighted the importance of the N-terminal helicase domain in DCL1 function. To gain mechanistic insight into the function of the helicase domain, we purified a truncated version of DCL1 by expressing it from a construct in which the sequence coding for the helicase domain had been deleted (DCL1Δhelicase; Fig. 5A; Supplemental Fig. S4B) and examined its in vitro processing activity (Fig. 5, B and C). Full-length DCL1 requires ATP for maximal in vitro processing activity (Fig. 5, B and C). By contrast, the processing activity of DCL1Δhelicase was unaffected by the absence of ATP (Fig. 5, B and C). We conclude that the DCL1 helicase domain is responsible for DCL1's ATP dependence.

Deletion of the helicase domain of human dicer, an ATP-independent dicer, enhances in vitro processing

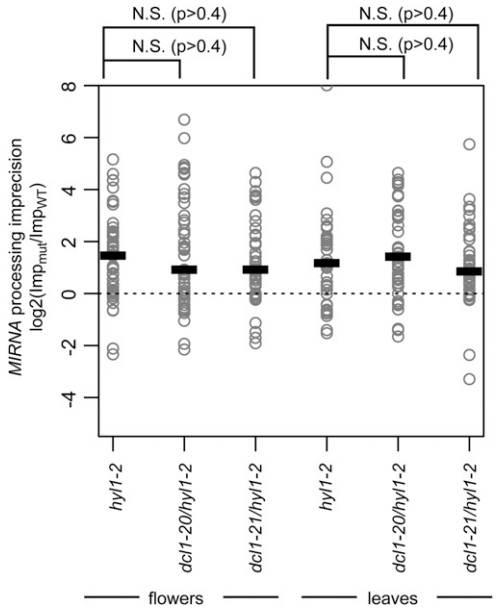

Figure 3. miRNA processing precision is not restored in *hyl1-2/dcl1* suppressor plants. The $\log_2$-transformed ratio of mutant imprecision/wild-type imprecision at each *MIRNA* hairpin was calculated for each possible mutant/wild-type combination. Only highly expressed hairpins were considered (top quartile in wild type). Values above zero indicate greater imprecision in the mutant compared to the wild type. Thick lines indicate median values. *P* values were derived from Kruskal-Wallis tests. N.S., Not significant.

activity (Ma et al., 2008). Similarly, the DCL1Δhelicase enzyme showed higher processing activity than full-length DCL1 both in the presence and in the absence of ATP when pri-miRNA156a RNA was used as the substrate (Fig. 5B). When pri-miRNA166b RNA was used as the substrate (Fig. 5C), the cleavage activity of DCL1Δhelicase was higher than that of full-length DCL1 only in the absence of ATP, albeit lower than that observed with full-length DCL1 in the presence of ATP.

We also compared the cleavage accuracy of DCL1 and DCL1Δhelicase by inspecting the distinct band patterns generated from precise cleavages. Precise cleavage of the pri-miRNA hairpin generates two arm fragments (F1, F2), miRNA/miRNA*(m/m*) fragments, and a loop fragment (F3; Fig. 5, D and E). We designed the substrate length so that the F1, F2, and F3 fragments have different lengths. As shown in Figure 5B, when pri-miRNA156a RNA was used as the substrate, there was no discernable difference in the cleavage accuracy between DCL1 and DCL1Δhelicase. However, when pri-miRNA166b RNA was used, a marked difference in processing accuracy was observed (Fig. 5C). Full-length DCL1 cleaved pri-miRNA166b accurately, generating the expected RNA fragments (Fig. 5C). In contrast, DCL1Δhelicase cleaved pri-miRNA166b less accurately, generating a ladder of fragments (Fig. 5C). Full-length DCL1 also generated a ladder of fragments in the absence of ATP (Fig. 5C). These results suggest that a functional helicase domain is required for the accurate processing for at least some pri-miRNA substrates.

Given the differential requirement for the helicase domain for pri-miRNA156a and pri-miRNA166b processing, we examined our smallRNAseq data to estimate the in vivo processing precision values at these loci. Increased imprecision at both loci was observed when comparing wild type to *hyl1-2* mutants, but the magnitude of the *hyl1-2* precision defect was dramatically higher for *MIR156a* relative to *MIR166b* (Fig. 5F). Both of the analyzed suppressed lines (*hyl1-2/dcl1-20* and *hyl1-2/dcl1-21*) had a partial alleviation of the *MIR156a* precision defect. In stark contrast, the imprecision in *MIR166b* processing was dramatically enhanced in the *hyl1-2/dcl1-20* and *hyl1-2/dcl1-21* lines relative to *hyl1-2* alone (Fig. 5F). Thus, both the in vitro and in vivo determinants of processing precision differ for these two hairpins. In the case of pri-miRNA156a, the helicase domain had no apparent effect on in vitro processing accuracy, and its removal enhanced the rate of processing; in vivo *MIR156a* was strongly dependent upon *hyl1-2* for processing precision. In contrast, for pri-miRNA166b, the maximal in vitro activity and processing accuracy was achieved only when the DCL1 helicase domain was present and provided with ATP; in vivo, *MIR166b* was much less dependent upon *hyl1-2* for processing precision and much more sensitive to the hyperactive DCL1 variants. The differences between these two substrates might

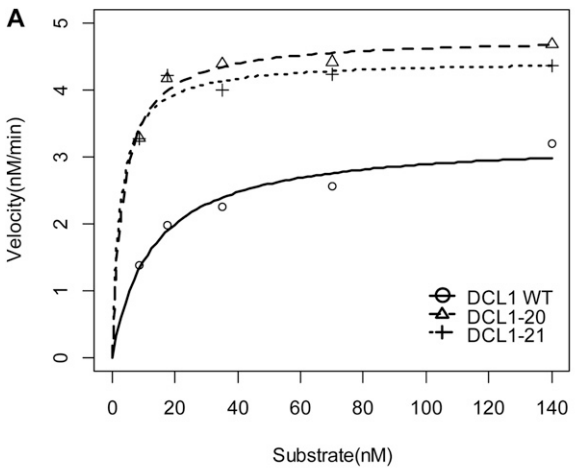

B

	Km(nM)	Kcat(min^{-1})	Kcat/Km(nM^{-1} min^{-1})
DCL1	12.71+/-0.04	0.361+/-0.001	0.028+/-0.000
DCL1-20	5.17+/-1.62	0.535+/-0.003	0.115+/-0.035
DCL1-21	3.60+/-1.01	0.491+/-0.003	0.148+/-0.043

Figure 4. Enhanced catalytic activity of suppressor DCL1 proteins. A, Reaction kinetics of pri-miRNA156a processed by DCL1, DCL1-20, and DCL1-21. B, Kinetic parameters of DCL1, DCL1-20, and DCL1-21.

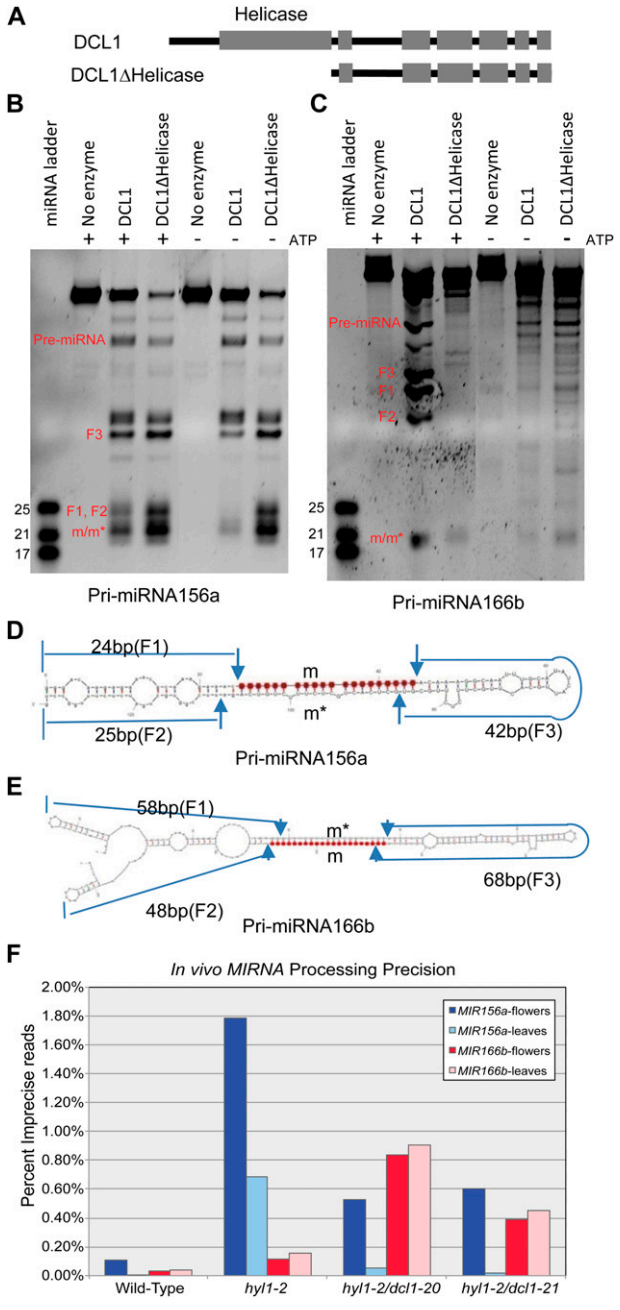

Figure 5. Cleavage of pri-miRNA156a and pri-miRNA166b by wild-type DCL1 and DCL1Δhelicase. A, Schematic diagram illustrating the DCL1ΔHelicase variant. B, Processing of pri-miRNA156a with or without ATP. C, Processing of pri-miRNA166b with or without ATP. D, The predicted secondary structure of pri-miRNA156a. Predicted fragments from precise DCL1-catalyzed processing are labeled as F1 and F2 (arm fragments), F3 (loop fragments), and m/m* (miRNA and miRNA* fragments). E, The predicted secondary structure of pri-miRNA 166b. Labeling conventions as in section D. F, In vivo *MIRNA* processing precision, estimated from smallRNAseq. The percentages of imprecise reads (i.e. those not within ±2 nucleotides of the annotated miRNA or miRNA*) are plotted for *MIR156a* and *MIR166b*.

reflect the accessibility of the different hairpin structures of the RNA substrates to the enzyme, and suggests a reciprocal relationship between reliance upon HYL1 and the DCL1 helicase domain for precision in *MIRNA* processing.

DCL1 Processes pri-miRNA Processively

Unlike mammalian dicers, which execute a single catalytic cycle to release miRNA/miRNA* duplexes from pre-miRNAs, miRNA/miRNA* duplex production by DCL1 involves at least two catalytic cycles (more for hairpins that produce multiple miRNA/miRNA* duplexes such as miR159 and miR319; Addo-Quaye et al., 2009; Bologna et al., 2009). To determine whether DCL1 executes these cleavages processively, we performed a single-cycle cleavage assay. An internally labeled pri-miRNA substrate (Fig. 6A) was preincubated with DCL1 in the absence of Mg^{2+} to allow the DCL1 to bind to the substrate without cleaving it, followed by addition of Mg^{2+} and unlabeled competitor substrate. If DCL1 cleavage is processive, addition of the unlabeled competitor substrates should have little effect on the production of mature 21-nt miRNA/miRNA*. As shown in Figure 6B, addition of a 1,000-fold excess of unlabeled substrate did not inhibit production of 21-nt products from the labeled substrates with which the enzyme was preincubated (compare lanes 3 and 4). By contrast, excess unlabeled substrate effectively inhibited production of labeled 21-nt products when preincubation was omitted (lane 5). These observations indicate that DCL1 cleaves pri-miRNA processively.

DISCUSSION

Increased DCL1 Activity Rescues the *hyl1* Phenotypes Despite Imprecise miRNA Biogenesis

As previously reported, *hyl1* plants exhibit lower levels of most miRNAs, resulting in the hyperaccumulation of some miRNA targets (Han et al., 2004; Vazquez et al., 2004). It is possible that, despite the broad impact of *hyl1* on the accumulation of most miRNAs, the *hyl1* phenotypes result primarily from dysregulation of just one or a small number of miRNA targets. Such a possibility is suggested by the observation that, despite a general impact on miRNA and other small RNA accumulation, the developmental anomalies caused by several viral suppressors of RNA silencing can be traced primarily to deregulation of a single miRNA target (Jay et al., 2011). Similarly, the embryonic lethality observed in *dcl1* null mutants, in which the accumulation of most miRNAs is severely reduced, appears to be due primarily to early patterning defects caused by precocious expression of just two miR156 targets (Nodine and Bartel, 2010). Genetic analyses indicate that dysregulation of the miR156, miR160, miR165/166, and miR319 pathways are particularly

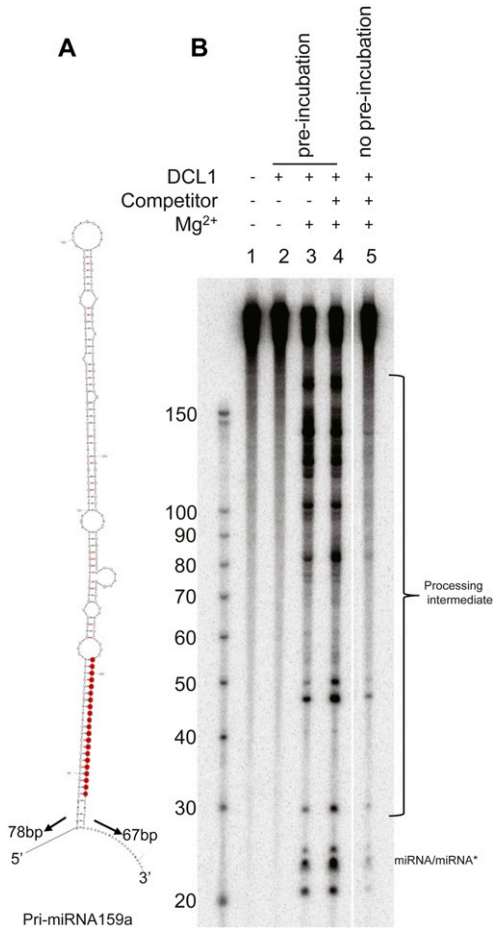

Figure 6. Processivity of DCL1 processing of pri-miRNA to miRNA. A, The secondary structure of pri-miRNA 159a. The mature miR159 is highlighted in black. B, Cleavage assays used an internally labeled pri-miRNA159a substrate and wild-type DCL1. DCL1 was preincubated with internally labeled substrate on ice and in the absence of Mg^{2+} in lanes 2 to 4. Processed RNAs were separated by urea-PAGE. [See online article for color version of this figure.]

relevant for the developmental phenotypes seen in *hyl1* mutants (Liu et al., 2011; Li et al., 2012). However, neither our *hyl1* suppressor screen nor a similar one reported by Tagami et al. (2009) identified any *MIRNA* or miRNA target loci as *hyl1* suppressors. Instead, the *hyl1* suppressor screens have only returned multiple alleles of *DCL1* that restore near wild-type levels of miRNA accumulation despite the absence of functional HYL1. While these screens are far from saturation, the available data suggest that the *hyl1* phenotypes are the result of multiple dysregulated miRNA targets, such that a broad and general recovery of miRNA accumulation levels, conditioned by heightened DCL1 activity, is required for phenotypic suppression.

The present biochemical characterization of the suppressor DCL1 proteins has shown that they process pri-miRNA more efficiently than wild-type DCL1, exhibiting both higher K_{cat} and lower K_m values in miRNA processing assays in vitro. Deep sequencing analysis of miRNA levels in vivo confirm that they are substantially elevated in the *dcl1/hyl1-2* plants compared with *hyl1-2* plants. Thus DCL1 variants with increased catalytic activity can compensate for a lack of HYL1 to produce quantities of mature miRNAs sufficient for normal development. In vitro and in vivo, HYL1 also enhances the precision of miRNA biogenesis (Kurihara et al., 2006; Dong et al., 2008). Our analysis of smallRNAseq data revealed that the fraction of imprecisely excised miRNA variants is higher for most *MIRNAs* in *hyl1-2* than in wild-type plants. Hence the *HYL1*-dependent precision in miRNA biogenesis affects many *MIRNAs*. miRNA processing precision was no better in the suppressor *dcl1/hyl1-2* plants than in the parental *hyl1-2* mutant plants. Taken together, these observations lead to the conclusion that the *dcl1* suppressor alleles compensate for the lack of *hyl1* function by increasing the rate, but not the fidelity, of miRNA biogenesis.

The RNaseIIIa and Helicase Domains of DCL1 in miRNA Processing

Together with another previously reported *hyl1-2* suppressor, *dcl1-13* (Tagami et al., 2009), there are now six *dcl1* alleles known to suppress the *hyl1* phenotypes. The corresponding mutations in the DCL1 protein are either in the helicase or RNaseIIIa domains and mutations in either domain give rise to mutant DCL1 proteins that suppress the *hyl1* phenotype by increasing DCL1 catalytic activity. Therefore the wild-type versions of these two DCL1 domains can be thought of as in some sense inhibitory. Suppressor mutations in the RNaseIIIa domain in all likelihood affect the catalytic properties of DCL1 directly, given their proximity to one of the two active sites of the protein. By contrast, suppressor mutations in the helicase domain are not close to the active sites and thus appear to have a more indirect role in modulating DCL1 activity.

The helicase domain of human Dicer has been reported to inhibit cleavage activity (Ma et al., 2008). It has been suggested that the human Dicer undergoes a conformational rearrangement during the activation of Dicer's catalytic activity and that the helicase domain functions as a structural switch to modulate cleavage activity (Ma et al., 2008). Generation of miRNA by animal dicers does not require the NTPase activity of the helicase domain (Zhang et al., 2002; Welker et al., 2011). Indeed, *Drosophila* Dicer-1, which is responsible for miRNA production, lacks a functional helicase domain altogether (Lee et al., 2004b). However, *Drosophila* Dicer-2 has a functional helicase domain and requires ATP to generate siRNAs from long dsRNA precursors (Liu et al., 2003). Mutations that abolish the NTPase activity of the helicase domain of *Caenorhabditis elegans* DCR-1 and human Dicer do not affect miRNA production, which commences with recognition of a substrate that has a 2-nt 3′ overhang and entails a single

cleavage, but abrogate siRNA production (Zhang et al., 2002; Welker et al., 2011). Recently, the *C. elegans* DCR1 and *Drosophila* Dicer-2 have been shown to recognize blunt-ended dsRNA substrates and cleave them processively to generate multiple internal siRNAs. The helicase domain has been proposed to function as an ATP-dependent translocase, providing the energy for translocation along the RNA substrate (Cenik et al., 2011; Welker et al., 2011). Thus the requirement for helicase activity is correlated with processivity and not catalysis per se.

In plants, DCL1 carries out both cleavages of the pri-miRNAs to release the miRNA/miRNA* duplex (Reinhart et al., 2002; Kurihara and Watanabe, 2004; Park et al., 2005; Fahlgren et al., 2007). Although purified Arabidopsis DCL1 alone is capable of cleaving pri-miRNAs, both the rate and precision of cleavage are enhanced by the HYL1 and SE proteins (Dong et al., 2008). The substrate structural features recognized by DCL1 have been defined to some extent (Mateos et al., 2010; Song et al., 2010; Werner et al., 2010), but neither the precise substrate recognition nor the cleavage mechanism is well understood. The present observations provide insight into the function of the DCL1 helicase domain, whose structure is that of a nucleic-acid-dependent NTPase (Lohman et al., 2008). Previous studies demonstrate that DCL1 activity is ATP dependent (Qi et al., 2005; Dong et al., 2008) and we showed here that ATP dependence is, indeed, associated with the helicase domain. However, elimination of the DCL1 helicase domain had markedly different outcomes with different substrates.

The initial cleavage of pri-miRNA156a in vitro is at the loop-proximal site (Supplemental Fig. S5). In the absence of ATP, miRNA release by the intact enzyme is markedly reduced and cleavage is confined primarily to the initial loop-proximal site (Fig. 5B). DCL1 lacking the helicase domain carries out both cuts efficiently. Hence the helicase domain inhibits DCL1 cleavage activity on this substrate primarily by affecting the second cleavage. Moreover, the observation that DCL1 cuts processively (Fig. 6) is consistent with the interpretation that ATP hydrolysis by the helicase domain promotes a conformational change necessary for the second cleavage to release the miRNA/miRNA* duplex. The enhanced activity of the suppressor variants *dcl1-20* and *dcl1-13* is likely to be attributable to inhibition or inactivation of the helicase domain by the mutations.

By contrast to what is observed with pri-miRNA156a, cleavage of pri-miRNA166b by native DCL1 is markedly lower in the absence of ATP than in the presence of ATP and only slightly elevated in the absence of ATP by elimination of the helicase domain. Moreover, cleavage of pri-miRNA166b by the intact enzyme is substantially less accurate in the absence of ATP than in its presence and is also less accurate if the DCL1 lacks the helicase domain. In vivo, the requirements for precise processing of *MIR156a* and *MIR166b* also differ: *MIR156a* is much more reliant upon HYL1 for processing precision when compared to *MIR166b*. Thus, our data suggest a reciprocal relationship between HYL1-dependent precision and DCL1-helicase domain-dependent precision during miRNA biogenesis, as well as variations in the relative importance of the two between different hairpins. It has been reported that the helicase domain of human Dicer is required for efficient processing of thermodynamically unstable hairpins while the cleavage of thermodynamically stable hairpin structures does not require the helicase domain (Soifer et al., 2008). Since HYL1 is known to colocalize with DCL1 in vivo and increase both its cleavage rate and accuracy (Kurihara et al., 2006; Fang and Spector, 2007; Song et al., 2007), it is likely to act on some substrates both to promote formation of the initial enzyme-substrate complex required for an accurate first cut and to activate a subsequent helicase-dependent conformational change required for the second cleavage. Whether its primary target is the substrate or DCL1 is the subject of current investigation.

MATERIALS AND METHODS

Plant Growth Conditions and Mutant Screen

All plants were grown under 12-h light/12-h dark cycle at approximately 21°C. *hyl1-2* (SALK_064863) mutant seeds were treated with 0.2% ethyl methane sulfonate for 16 h. After extensive washing with water, seeds were sown on soil. Seedling phenotypes were evaluated after two weeks. Plants that clearly showed the *hyl1-2* mutant phenotypes were removed and the remaining plants were grown for another 3 weeks, then reevaluated for plants exhibiting wild-type phenotypes.

Cloning and Complementation of the Mutant Alleles

The genomic sequences at the *DCL1* locus were PCR amplified to produce three overlapping fragments. PCR fragments were sequenced to identify the mutated sites. To obtain the promoter of *DCL1*, a genomic fragment containing 1,617-bp upstream from translation start site (gene model AT1G01040.1) and a 1,730-bp fragment containing the coding sequence were amplified using primers DCL1_Pro_F and DCL1_Pro_R and cloned into the PCR2.1-TOPO vector (Invitrogen) to generate PCR2.1-promoter vectors (see Supplemental Table S1). To obtain the mutant versions of *DCL1*, the relevant fragment from *dcl1-20* was amplified from *dcl1-20* genomic DNA, while the mutations identified in *dcl1-21*, *dcl1-22*, *dcl1-23*, and *dcl1-24* were generated by overlapping PCR in the pENTR-DCL1-FLAG vector (Dong et al., 2008). The promoters were excised from the PCR2.1-promoter vector using *Not*I and *Xho*I and cloned into pENTR-DCL1-FLAG vector cut with the same pair of restriction enzymes. Finally, the *DCL1* promoter-driven DCL1-FLAG expression cassettes were cloned into pEarleyGate 302 by GATEWAY technology. The resulting constructs were used to transform *hyl1-2* plants.

Quantitative Real-Time PCR

Approximately 50 mg of rosette leaf tissue from 25-d plants, grown under long-day conditions (16-h/8-h light/darkness) at approximately 20°C was harvested and used for total RNA extraction with the miRNeasy kit (Qiagen) per the manufacturer's instructions. Tissue from transgenic P^{DCL1}:*dcl1* plants was from a pooled mixture of herbicide-resistant T2 individuals, all of which had complemented that *hyl1-2* phenotype. Total RNA was treated with RNase-free DNaseI (Fermentas) per the manufacturer's instructions. For mRNA analysis, 435 ng of DNase-treated RNA was used for first-strand cDNA synthesis using oligo$(dT)_{(20)}$ using Superscript III supermix (Invitrogen/Life Technologies) in 10 μL reactions. Primers for *DCL1* (At1g01040) and

ACTIN2 (At3g18780) were used in SYBR-green I PCR reactions (Fermentas) conducted in a Step-One Plus instrument (ABI/Life Technologies), with four samples per genotype (two biological replicates × two technical replicates). The *DCL1* forward primer spanned the miR162 target site at the exon 12-13 junction, and the *DCL1* reverse primer spanned the exon 14-15 junction, thus ensuring that only intact *DCL1* cDNA was measured. Mean PCR efficiencies for each primer set were calculated using LinRegPCR (Ruijter et al., 2009) and used to calculate the *DCL1* accumulation, using *ACTIN2* as a reference, relative to the mean Columbia-0 value as described (Pfaffl, 2001). miRNA analysis used 145 ng of DNase-treated total RNA in stem-loop primer-mediated reverse transcription as described (Varkonyi-Gasic and Hellens, 2010), except that a 1 μM mixture of oligos, consisting of 0.495 μM stem-loop miR162, 0.495 μM miR838, and 0.01 μM U6, was used for reverse transcription. Primers for ath-miR162a, ath-miR838, and *U6* were used in SYBR-green I PCR reactions (Fermentas) as described above. Data analysis was as described above except that *U6* was used as the reference.

miRNA Northern-Blot Analysis

Total RNA was extracted from leaves of 5-week-old plants and flowers of 8-week-old plants by the Trizol method. Ten micrograms of total RNA was separated on a 12% SequaGel (National Diagnostics) and blotted to Hybond N^+ membrane (Amersham). Hybridization and detection was performed as described by Han et al. (2004).

SmallRNAseq

Total RNA was extracted from 5-week-old leaves and 8-week-old flowers. Total RNAs were sent to the Genomics Core Facility of the Pennsylvania State University at University Park. Small RNA libraries were prepared and sequenced using SOLiD technology by following the standard instructions of the manufacturer (ABI). The small RNA reads were trimmed by in-house Perl scripts and mapped to the miRNA hairpin sequences downloaded from mirRBase (http://www.mirbase.org, Arabidopsis version 16) using the Bowtie program (Langmead et al., 2009). Mapped reads were analyzed and plotted using custom Perl and Python scripts and the R software package. The relevant data have been deposited at the National Center for Biotechnology Information (Gene Expression Omnibus, accession no. GSE29802). Comparisons of miRNA/miRNA* accumulation (Fig. 2C) and miRNA processing precision (Fig. 3) used the Kruskal-Wallis one-way ANOVA to test for significant differences in median values between two nonnormally distributed population.

Protein Expression and Purification

All versions of *DCL1* were generated by overlap PCR in pENTR-DCL1-FLAG vector (Dong et al., 2008) and then cloned into pDEST10 vector to obtain the pDEST10-DCL1-FLAG vectors. Bacmids were generated by transforming DH10Bac cells (Invitrogen) with pDEST10-DCL1-FLAG vectors. Protein expression and purification were performed essentially as described by Dong et al. (2008).

In Vitro miRNA Processing

Genomic fragments containing pri-miRNA156a and pri-miRNA166b were amplified using primer sets pri-156a-T7 and pri-156a-R and pri-166b-T7 and pri-166b-R, respectively. The resulting 133- and 216-bp PCR fragments were gel purified and used as the templates to synthesize RNA substrates. RNA substrates were synthesized using the Megascript T7 kit (Ambion, AM1334). The miRNA processing activity assay was performed as described in Dong et al. (2008). To measure the initial velocity of DCL1 enzymes, RNAs 5′ labeled with γ P^{32} ATP using the KinaseMax kit (Ambion, AM1520) were used as substrates. Ten-microliter reactions were allowed to proceed for 5 min and stopped by adding 100 μL stopping buffer (0.3 M sodium acetate, 0.1% SDS, and 5 mM EDTA). The RNAs were acid-phenol extracted and precipitated using GylcoBlue (Ambion, AM9515). Precipitated RNA was resuspended in 10 μL gel loading buffer (Ambion, AM8547) and separated on an 8% SequaGel (National Diagnostics). Gels were dried using a Biorad model 583 gel dryer and exposed to a PhosphorImager screen over night. Images were acquired on a Typhoon 9410 and quantified using ImageJ software. The kinetics constants were calculated by fitting the data using a nonlinear least squares model in the R software package (Ma et al., 2008).

Single Cycle Cleavage Assay

The template for pri-miRNA159a RNA synthesis was prepared as described above using primers pri-159a-T7 and pri-159a-R. Internally ^{32}P-labeled pri-miRNA 159 RNA was synthesized using a MAXIscript T7 kit (Ambion, AM1314) and gel purified. Unlabeled pri-miRNA 159a RNA was synthesized using a Megascript T7 kit (Ambion, AM1334). A total of 65 pg of the labeled substrates were preincubated with DCL1 (20 ng) on ice for 15 min in reaction buffer without Mg^{2+}. The reactions were then transferred to room temperature for another 15 min. Water (negative control), $MgCl_2$ (4 mM final concentration), or $MgCl_2$ with 100 ng cold substrates was added to the reactions. A reaction from which the preincubation step was omitted was set up by mixing labeled substrate with cold substrate first and then adding the DCL1 to initiate cleavage. All reactions were in 10 μL total volume and incubated for 6 min. The reactions were stopped by adding 100 μL stopping buffer. RNA were extracted and separated as described above.

SmallRNAseq data were deposited to the National Center for Biotechnology Information GEO (GSE29802).

Supplemental Data

The following materials are available in the online version of this article.

Supplemental Figure S1. Multiple sequence alignment of the helicase and RNAseIIIa domains of DCL1, DCL2, DCL3, and DCL4 in Arabidopsis Arabidopsis (*Arabidopsis thaliana*; At), rice (*Oryza sativa*; Os), moss (*Physcomitrella patens*; Pp), and poplar (*Populus trichocarpa*; Pt).

Supplemental Figure S2. Molecular models of the helicase and RNaseIIIa domains of DCL1.

Supplemental Figure S3. miRNA accumulation in the dcl1/HYL1 background.

Supplemental Figure S4. Purification of recombinant DCL1 proteins.

Supplemental Figure S5. The cleavage of pri-by DCL1, DCL1-20, and DCL1-21.

Supplemental Table S1. Oligonucleotide sequences.

ACKNOWLEDGMENTS

We thank Dr. Craig Praul and the staff of the Genomics Core Facility of the Pennsylvania State University at University Park for providing smallRNAseq services. C.L. and N.V.F. designed the research. C.L. performed the research. M.J.A. analyzed smallRNAseq data. C.L., M.J.A., and N.V.F. wrote the article. All authors contributed to revising the draft manuscript and approved the final version.

Received January 9, 2012; accepted March 30, 2012; published April 3, 2012.

LITERATURE CITED

Addo-Quaye C, Snyder JA, Park YB, Li Y-F, Sunkar R, Axtell MJ (2009) Sliced microRNA targets and precise loop-first processing of MIR319 hairpins revealed by analysis of the *Physcomitrella patens* degradome. RNA **15:** 2112–2121

Allen E, Xie Z, Gustafson AM, Carrington JC (2005) microRNA-directed phasing during trans-acting siRNA biogenesis in plants. Cell **121:** 207–221

Bologna NG, Mateos JL, Bresso EG, Palatnik JF (2009) A loop-to-base processing mechanism underlies the biogenesis of plant microRNAs miR319 and miR159. EMBO J **28:** 3646–3656

Borsani O, Zhu J, Verslues PE, Sunkar R, Zhu JK (2005) Endogenous siRNAs derived from a pair of natural cis-antisense transcripts regulate salt tolerance in Arabidopsis. Cell **123:** 1279–1291

Cenik ES, Fukunaga R, Lu G, Dutcher R, Wang Y, Tanaka Hall TM, Zamore PD (2011) Phosphate and R2D2 restrict the substrate specificity of Dicer-2, an ATP-driven ribonuclease. Mol Cell **42:** 172–184

Dong Z, Han MH, Fedoroff N (2008) The RNA-binding proteins HYL1 and SE promote accurate *in vitro* processing of pri-miRNA by DCL1. Proc Natl Acad Sci USA **105:** 9970–9975

Dunoyer P, Brosnan CA, Schott G, Wang Y, Jay F, Alioua A, Himber C, Voinnet O (2010) An endogenous, systemic RNAi pathway in plants. EMBO J **29:** 1699–1712

Fahlgren N, Howell MD, Kasschau KD, Chapman EJ, Sullivan CM, Cumbie JS, Givan SA, Law TF, Grant SR, Dangl JL, et al (2007) High-throughput sequencing of Arabidopsis microRNAs: evidence for frequent birth and death of MIRNA genes. PLoS ONE **2:** e219

Fang Y, Spector DL (2007) Identification of nuclear dicing bodies containing proteins for microRNA biogenesis in living Arabidopsis plants. Curr Biol **17:** 818–823

Han MH, Goud S, Song L, Fedoroff N (2004) The Arabidopsis double-stranded RNA-binding protein HYL1 plays a role in microRNA-mediated gene regulation. Proc Natl Acad Sci USA **101:** 1093–1098

Hutvágner G, Zamore PD (2002) A microRNA in a multiple-turnover RNAi enzyme complex. Science **297:** 2056–2060

Jay F, Wang Y, Yu A, Taconnat L, Pelletier S, Colot V, Renou JP, Voinnet O (2011) Misregulation of AUXIN RESPONSE FACTOR 8 underlies the developmental abnormalities caused by three distinct viral silencing suppressors in Arabidopsis. PLoS Pathog **7:** e1002035

Kasschau KD, Xie Z, Allen E, Llave C, Chapman EJ, Krizan KA, Carrington JC (2003) P1/HC-Pro, a viral suppressor of RNA silencing, interferes with Arabidopsis development and miRNA unction. Dev Cell **4:** 205–217

Kim S, Yang JY, Xu J, Jang IC, Prigge MJ, Chua NH (2008) Two cap-binding proteins CBP20 and CBP80 are involved in processing primary microRNAs. Plant Cell Physiol **49:** 1634–1644

Kurihara Y, Takashi Y, Watanabe Y (2006) The interaction between DCL1 and HYL1 is important for efficient and precise processing of pri-miRNA in plant microRNA biogenesis. RNA **12:** 206–212

Kurihara Y, Watanabe Y (2004) Arabidopsis micro-RNA biogenesis through Dicer-like 1 protein functions. Proc Natl Acad Sci USA **101:** 12753–12758

Langmead B, Trapnell C, Pop M, Salzberg SL (2009) Ultrafast and memory-efficient alignment of short DNA sequences to the human genome. Genome Biol **10:** R25

Laubinger S, Sachsenberg T, Zeller G, Busch W, Lohmann JU, Rätsch G, Weigel D (2008) Dual roles of the nuclear cap-binding complex and SERRATE in pre-mRNA splicing and microRNA processing in Arabidopsis thaliana. Proc Natl Acad Sci USA **105:** 8795–8800

Lee Y, Ahn C, Han J, Choi H, Kim J, Yim J, Lee J, Provost P, Rådmark O, Kim S, et al (2003) The nuclear RNase III Drosha initiates microRNA processing. Nature **425:** 415–419

Lee Y, Kim M, Han J, Yeom KH, Lee S, Baek SH, Kim VN (2004a) MicroRNA genes are transcribed by RNA polymerase II. EMBO J **23:** 4051–4060

Lee YS, Nakahara K, Pham JW, Kim K, He Z, Sontheimer EJ, Carthew RW (2004b) Distinct roles for Drosophila Dicer-1 and Dicer-2 in the siRNA/miRNA silencing pathways. Cell **117:** 69–81

Li S, Yang X, Wu F, He Y (January 20, 2012) HYL1 controls the miR156-mediated juvenile phase of vegetative growth. J Exp Bot http://dx.doi.org/10.1093/jxb/err465

Liu QH, Rand TA, Kalidas S, Du FH, Kim HE, Smith DP, Wang XD (2003) R2D2, a bridge between the initiation and effector steps of the Drosophila RNAi pathway. Science **301:** 1921–1925

Liu Z, Jia L, Wang H, He Y (2011) HYL1 regulates the balance between adaxial and abaxial identity for leaf flattening via miRNA-mediated pathways. J Exp Bot **62:** 4367–4381

Lobbes D, Rallapalli G, Schmidt DD, Martin C, Clarke J (2006) SERRATE: a new player on the plant microRNA scene. EMBO Rep **7:** 1052–1058

Lohman TM, Tomko EJ, Wu CG (2008) Non-hexameric DNA helicases and translocases: mechanisms and regulation. Nat Rev Mol Cell Biol **9:** 391–401

Lu C, Fedoroff N (2000) A mutation in the *Arabidopsis* HYL1 gene encoding a dsRNA binding protein affects responses to abscisic acid, auxin, and cytokinin. Plant Cell **12:** 2351–2366

Lund E, Dahlberg JE (2006) Substrate selectivity of exportin 5 and Dicer in the biogenesis of microRNAs. Cold Spring Harb Symp Quant Biol **71:** 59–66

Ma E, MacRae IJ, Kirsch JF, Doudna JA (2008) Autoinhibition of human dicer by its internal helicase domain. J Mol Biol **380:** 237–243

Mateos JL, Bologna NG, Chorostecki U, Palatnik JF (2010) Identification of microRNA processing determinants by random mutagenesis of Arabidopsis MIR172a precursor. Curr Biol **20:** 49–54

Mlotshwa S, Schauer SE, Smith TH, Mallory AC, Herr JM Jr, Roth B, Merchant DS, Ray A, Bowman LH, Vance VB (2005) Ectopic DICER-LIKE1 expression in P1/HC-Pro *Arabidopsis* rescues phenotypic anomalies but not defects in microRNA and silencing pathways. Plant Cell **17:** 2873–2885

Nodine MD, Bartel DP (2010) MicroRNAs prevent precocious gene expression and enable pattern formation during plant embryogenesis. Genes Dev **24:** 2678–2692

Park MY, Wu G, Gonzalez-Sulser A, Vaucheret H, Poethig RS (2005) Nuclear processing and export of microRNAs in Arabidopsis. Proc Natl Acad Sci USA **102:** 3691–3696

Pfaffl MW (2001) A new mathematical model for relative quantification in real-time RT-PCR. Nucleic Acids Res **29:** e45

Qi Y, Denli AM, Hannon GJ (2005) Biochemical specialization within Arabidopsis RNA silencing pathways. Mol Cell **19:** 421–428

Qin H, Chen F, Huan X, Machida S, Song J, Yuan YA (2010) Structure of the Arabidopsis thaliana DCL4 DUF283 domain reveals a noncanonical double-stranded RNA-binding fold for protein-protein interaction. RNA **16:** 474–481

Rajagopalan R, Vaucheret H, Trejo J, Bartel DP (2006) A diverse and evolutionarily fluid set of microRNAs in *Arabidopsis thaliana*. Genes Dev **20:** 3407–3425

Reinhart BJ, Weinstein EG, Rhoades MW, Bartel B, Bartel DP (2002) MicroRNAs in plants. Genes Dev **16:** 1616–1626

Rocak S, Linder P (2004) DEAD-box proteins: the driving forces behind RNA metabolism. Nat Rev Mol Cell Biol **5:** 232–241

Ruijter JM, Ramakers C, Hoogaars WMH, Karlen Y, Bakker O, van den Hoff MJB, Moorman AFM (2009) Amplification efficiency: linking baseline and bias in the analysis of quantitative PCR data. Nucleic Acids Res **37:** e45

Schauer SE, Jacobsen SE, Meinke DW, Ray A (2002) DICER-LIKE1: blind men and elephants in Arabidopsis development. Trends Plant Sci **7:** 487–491

Soifer HS, Sano M, Sakurai K, Chomchan P, Saetrom P, Sherman MA, Collingwood MA, Behlke MA, Rossi JJ (2008) A role for the Dicer helicase domain in the processing of thermodynamically unstable hairpin RNAs. Nucleic Acids Res **36:** 6511–6522

Song L, Axtell MJ, Fedoroff NV (2010) RNA secondary structural determinants of miRNA precursor processing in Arabidopsis. Curr Biol **20:** 37–41

Song L, Han MH, Lesicka J, Fedoroff N (2007) Arabidopsis primary microRNA processing proteins HYL1 and DCL1 define a nuclear body distinct from the Cajal body. Proc Natl Acad Sci USA **104:** 5437–5442

Tagami Y, Motose H, Watanabe Y (2009) A dominant mutation in DCL1 suppresses the *hyl1* mutant phenotype by promoting the processing of miRNA. RNA **15:** 450–458

Varkonyi-Gasic E, Hellens RP (2010) qRT-PCR of small RNAs. Methods Mol Biol **631:** 109–122

Vazquez F, Gasciolli V, Crété P, Vaucheret H (2004) The nuclear dsRNA binding protein HYL1 is required for microRNA accumulation and plant development, but not posttranscriptional transgene silencing. Curr Biol **14:** 346–351

Welker NC, Maity TS, Ye X, Aruscavage PJ, Krauchuk AA, Liu Q, Bass BL (2011) Dicer's helicase domain discriminates dsRNA termini to promote an altered reaction mode. Mol Cell **41:** 589–599

Werner S, Wollmann H, Schneeberger K, Weigel D (2010) Structure determinants for accurate processing of miR172a in Arabidopsis thaliana. Curr Biol **20:** 42–48

Willmann MR, Mehalick AJ, Packer RL, Jenik PD (2011) MicroRNAs regulate the timing of embryo maturation in Arabidopsis. Plant Physiol **155:** 1871–1884

Xie Z, Kasschau KD, Carrington JC (2003) Negative feedback regulation of *Dicer-Like1* in *Arabidopsis* by microRNA-guided mRNA degradation. Curr Biol **13:** 784–789

Yang L, Liu Z, Lu F, Dong A, Huang H (2006) SERRATE is a novel nuclear regulator in primary microRNA processing in Arabidopsis. Plant J **47:** 841–850

Yi R, Qin Y, Macara IG, Cullen BR (2003) Exportin-5 mediates the nuclear export of pre-microRNAs and short hairpin RNAs. Genes Dev **17:** 3011–3016

Yu B, Bi L, Zheng B, Ji L, Chevalier D, Agarwal M, Ramachandran V, Li W, Lagrange T, Walker JC, et al (2008) The FHA domain proteins DAWDLE in Arabidopsis and SNIP1 in humans act in small RNA biogenesis. Proc Natl Acad Sci USA **105:** 10073–10078

Zhang H, Kolb FA, Brondani V, Billy E, Filipowicz W (2002) Human Dicer preferentially cleaves dsRNAs at their termini without a requirement for ATP. EMBO J **21:** 5875–5885